AAS 16-348

ATTITUDE DETERMINATION AND CONTROL OF ITASAT CUBESAT

Valdemir Carrara*

The ITASAT CubeSat is a satellite being developed at Aeronautic Technological Institute in Brazil, to be launched in mid-2016. This work addresses the ADCS (Attitude Determination and Control Subsystem) of ITASAT, and the computer simulation done so far to assure that the mission requirements were accomplished. The formulation of a Kalman filter will be presented to estimate the attitude quaternion along with the gyro bias, having as inputs the raw measurements of the magnetometer and gyroscopes, and a preprocessed vector of coarse cosine sun sensors. The formulation shown here was taken from an algorithm of a similar Kalman filter, but adapted for employment on on-board computers in which unnecessary computations were eliminated. Attitude is estimated during the illuminated part of the orbit, based on measurements of the angular sensors. During eclipse attitude estimation procedure relies only on the magnetometer and gyros measurements, but the estimation error increases with the time the satellite remains in the shadow due to the lack of sun sensor readings necessary for full attitude estimation. Preliminary results indicate that the Kalman filter can track the bias of the gyroscope and its drift, significantly decreasing the noise level present in the angular sensors. However, the angular velocity remains with high noise levels, which restricts the use of the gyroscope to drive the control signal without previous filtering. The ITASAT should be stabilized and controlled in three-axis, with geocentric pointing. A set of three reaction wheels and three magnetorquers provide torques for attitude control. Simulations indicated that the pointing accuracy is particularly affected by the Kalman filter estimation error, when the reaction wheels are used as main actuators. However, due to the high power consumption of the wheels they can not be used during the whole orbit, and therefore a purely three-axis magnetic stabilization and control will also be required. The magnetorquer's inability to generate torques in all directions limits the attitude stabilization of this control. Coupled to the poor resolution of the angular velocity from gyros, pointing errors bellow 20 degrees are difficult to achieve, except when the angular velocity is estimated by other means such as, for example, by gyro filtering, or by numeric attitude derivative. The ITASAT attitude control modes will be presented, together with some simulation results.

* Dr., Instituto Tecnológico da Aeronáutica, DCTA, P. Marechal Eduardo Gomes, 50, S. J. dos Campos, SP, Brazil.

INTRODUCTION

The ever increasing number of launched CubeSats brought back searching of improving methods for attitude determination and estimation based on two vectors, which had been forgotten after star sensors have become widely available on satellites. Although there are also commercially available star sensors for CubeSats, their use has not yet been widespread, perhaps due to their cost compared to the well established group formed by sun sensor, magnetometers and gyroscopes based on MEMS (Micro-Electrico-Mechanical System) technology. MEMS gyroscopes lack the resolution needed to increase the accuracy of the estimated attitude, but they can still be used in estimation procedures based on Kalman filter, provided their biases are also estimated in flight. Algorithms like TRIAD[1, 2, 3] and QUEST[3, 4, 5] employ deterministic algorithms to compute the attitude based on two observed vectors. Stochastic attitude estimation proved to be efficient when sensor noise is significant[6, 7]. Additionally, several researches have been conducted showing the effectiveness of attitude estimation based on two vectors and rate measurement[8, 9], applied not only to satellites but also in UAVs (Unmanned Autonomous Vehicle) and drones[10].

The ITASAT is a 6U (2×3) CubeSat nano-satellite scheduled to be launched in mid-2016. Its ADCS (Attitude Determination and Control Subsystem) is composed by a set of MEMS gyroscopes, three-axis magnetometer (TAM) and six coarse Sun sensors (CSS), providing full coverage of the Sun direction. An onboard computer based on a ARM-7 32-bit computer will perform sensor data acquisition, attitude determination and control, besides managing the attitude operating modes and wealthy monitoring. The ADCS will count also with three reaction wheels (RW) and three magnetic torquers (MT) aligned to the satellite axes. The main purpose of ITASAT is to relay environmental data collected by autonomous platforms spread in the country to mission center.

This work will describe the ITASAT attitude estimation techniques, its control laws and some results from simulation of the attitude control. A Kalman filter with reduced order covariance matrix was adopted for attitude estimation[9], with an optimized formulation proper for onboard implementation. Next sections will describe the ADCS operating modes, the Kalman filter, the control laws for the operating modes and some results from attitude control simulation.

ATTITUDE CONTROL OPERATING MODES

The ITASAT CubeSat will be three-axis stabilized with magnetic torque coils (MT) and reaction wheels (RW) operating with null nominal angular momentum. In nominal mode the satellite shall be Earth referenced, that means that one of its axis will point to the Earth's center. The satellite coordinate system is shown in Figure 1. In nominal attitude the x-axis will point to Nadir (up direction), and the z-axis to the normal to the orbit plane. The y-axis completes the frame and is approximately parallel to the satellite velocity v with respect to Earth. This coordinate system is called orbital or reference system, while the satellite coordinate system will be referenced by body fixed frame.

The ADCS will require four attitude control modes. Just after orbit injection the satellite automatically enters in Safe Mode (SM), where the attitude remains uncontrolled. This mode allows sending ground commands to the satellite and receiving the onboard telemetry. In this mode the sensors and actuators are switched off. From the SM the satellite can be commanded to switch to Attitude Stabilization Mode (ASM) or alternatively to the Attitude Determination and Estimation mode (ADE), as shown in Figure 2. The ADE is not a real operating mode, since attitude determination and estimation are also done in all modes, except the Safe Mode. The ADE was considered an operating mode due to the necessity of attitude knowledge even when the attitude is not being stabilized or controlled, and also to have time for filter convergence.

Moreover, by checking the attitude determination error from telemetry (by means of the filter residue, for instance), the attitude control modes can be activated without taking risk of attitude instability. The ASM will employ a B-dot[11] or a Rate Reduction algorithm to stabilize the satellite and to reduce its angular velocity. The Rate Reduction method is similar to the B-dot, but it uses the gyroscope measurements for satellite de-spun instead of the time derivative of the magnetometer outputs employed by the B-dot. The connecting lines and arrows in Figure 2 show the ground commands to switch to and from the operating modes.

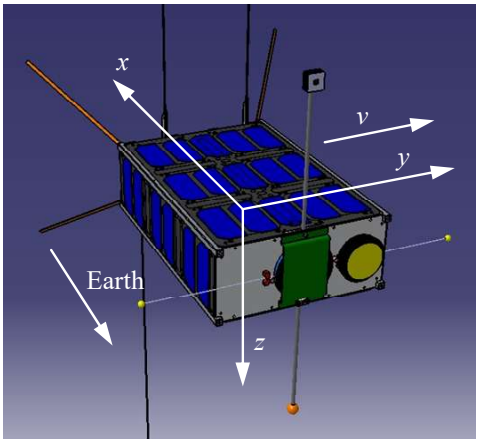

Figure 1. ITASAT's body fixed axes.

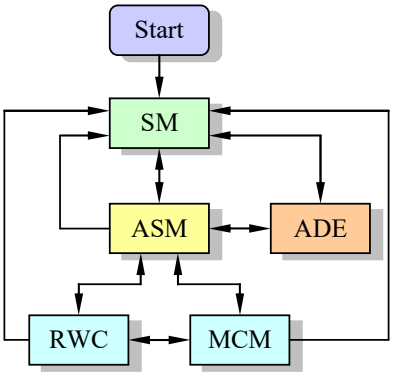

Figure 2. ADCS operating modes.

In Attitude Determination and Estimation mode the procedures to perform both attitude determination and estimation will be carried out. The main module is a Kalman filter to estimate the attitude based on the sensor readings, as will be detailed in next section. However, alternatively a TRIAD[1] or a QUEST[4] algorithm can be used to provide attitude determination. When the satellite is operating in ADE mode, all the actuators are switched off and no actions on attitude control are performed. Two conditions are needed to allow switching to nominal mode: the attitude shall be known with high confidence and the satellite angular rate shall be small. The ADE mode provides the first condition of attitude estimation error and the last condition is

achieved by the ASM mode. In the ASM the satellite angular rate shall be damped from 60°/s at satellite deployment till a maximum specified value of 0.6°/s in any axis.

Two nominal modes are envisaged for Earth pointing: Reaction Wheel Control mode (RWC) and Magnetic Control Mode (MCM). The RWC will rely on a conventional PID (Proportional, Integral and Derivative) with gains adjusted to drive the reaction wheels whenever an attitude error is detected. The angular rate is also adjusted to track the orbital rate, around 0.06°/s, as the satellite travels its orbit. Reaction wheel angular momentum will be damped by means of magnetic torques, in order to maintain the RW speed in a safe range. The second control law is a three-axis Magnetic Control Mode which also uses a PID control based exclusively on the magnetic torque coils to drive the satellite attitude. Due to the small torque provided by this type of actuator, it is expected that the attitude error will be larger than RWC. Moreover, the inability of the MT to generate torques in three-axis can jeopardize this type of control, and makes gain tuning a really difficult task. These two types of controllers are needed due to the energy restrictions for operating the RW during the whole orbit. It is expected that the satellite will operate in RWC when contact with the mission center is established and in MCM whenever it is out of contact with ground station. At any operating mode the satellite can be automatically switched to Safe Mode by onboard failure detection algorithms, which monitors the attitude to detect anomalies. These anomalies are signalized to on-ground specialists and actions are taken in order to overcome the problem, if any. Next sections will present respectively the Attitude Determination and Estimation mode, the Reaction Wheel Control mode, the three-axis Magnetic Control Mode and the Attitude Stabilization Mode of ITASAT.

ATTITUDE DETERMINATION AND ESTIMATION

The ADE mode is composed of the TRIAD and QUEST attitude determination algorithms[1, 4], and a Kalman filter with reduced order covariance matrix[9]. The determination or estimation methods are selectable by ground command. Attitude is determined or estimated based in two vectors measured by the magnetometer and coarse sun sensors. When in the Earth's shadow the attitude determination methods can't detect the real attitude due to the lack of the sun vector and, therefore, delivers the reference attitude so the control remains inactive. On the other hand the Kalman filter can still improve the attitude estimation with the measures of the magnetometer only, although with larger error. The reduced order Kalman filter will be formulated in sequence, optimized for onboard computation. The equations for the attitude determination methods can be found in the mentioned references.

Sensor Models

The gyroscope was modeled as being composed by the measured angular rate vector, $\boldsymbol{\omega}$, added to a Gaussian white noise and bias:

$$\boldsymbol{\omega}_g = \boldsymbol{\omega} + \mathbf{b} + \boldsymbol{\eta}, \tag{1}$$

where $\boldsymbol{\eta}$ is a white noise with zero mean and covariance matrix $\mathbf{N}$. The bias $\mathbf{b}$ is not constant, because gyros in general exhibit a bias drift which can be modeled as

$$\dot{\mathbf{b}} = \boldsymbol{\mu}, \tag{2}$$

with $\boldsymbol{\mu}$ being also a Gaussian white noise with zero mean and covariance $\mathbf{M}$, uncorrelated with $\boldsymbol{\eta}$. The standard deviation of $\boldsymbol{\mu}$ is associated with the gyroscope bias instability. It is assumed that the bias dynamics can be discretized in time by

$$\mathbf{b}_k = \mathbf{b}_{k-1} + \boldsymbol{\mu}\, \mathrm{d}t\,, \tag{3}$$

where $\mathrm{d}t = t_k - t_{k-1}$ is the time interval between two consecutive gyro measures. The standard deviations associated with **N** and **M** were obtained by comparing the Allan variance[12, 13] of the mathematical model with data provided by the gyroscope supplier. Scale factor errors and axis misalignments of all sensors were taken into account in the simulation, assuming typical values found in MEMS sensors. The magnetometer (TAM) and coarse sun sensors (CSS) models consider only an additive Gaussian white noise. It was assumed also that any magnetic remnant dipole on the satellite can be mitigated during satellite integration. However, an attitude disturbance caused by a constant dipole of 0.0001 Am^2 on the satellite was considered in simulation, although the dipole influence on the magnetometer bias was disregarded. The effect of the Earth's albedo on the CSS was not taken into account in the simulation. The albedo can cause an error on the sensor similar to a slow changing bias.

Attitude Motion

The satellite is considered as a rigid body with reaction wheels. In terms of the Euler symmetric parameters the kinematics is given by[9, 14, 15]

$$\dot{\mathbf{q}} = \frac{1}{2}\boldsymbol{\Omega}(\boldsymbol{\omega})\,\mathbf{q}\,, \tag{4}$$

where $\mathbf{q} = (\boldsymbol{\varepsilon}, \eta)$ is the attitude quaternion ($\boldsymbol{\varepsilon}$ is the vector and η is the scalar component), $\boldsymbol{\omega}$ is the satellite angular velocity and $\boldsymbol{\Omega}$ is the extended cross product matrix, given by

$$\boldsymbol{\Omega}(\boldsymbol{\omega}) = \begin{bmatrix} -\boldsymbol{\omega}^{\times} & \boldsymbol{\omega} \\ -\boldsymbol{\omega}^{\mathrm{T}} & 0 \end{bmatrix}, \tag{5}$$

where the superscript T means the transposed vector, and $\times$ represents the cross product matrix:

$$\boldsymbol{\omega}^{\times} = \begin{bmatrix} 0 & -\omega_3 & \omega_2 \\ \omega_3 & 0 & -\omega_1 \\ -\omega_2 & \omega_1 & 0 \end{bmatrix}. \tag{6}$$

The kinematics can be equivalently expressed as

$$\dot{\mathbf{q}} = \frac{1}{2}\boldsymbol{\Xi}(\mathbf{q})\,\boldsymbol{\omega}\,, \tag{7}$$

in which $\boldsymbol{\Xi}(\mathbf{q})$ is given by[9]

$$\boldsymbol{\Xi}(\mathbf{q}) = \begin{bmatrix} \eta & -\varepsilon_3 & \varepsilon_2 \\ \varepsilon_3 & \eta & -\varepsilon_1 \\ -\varepsilon_2 & \varepsilon_1 & \eta \\ -\varepsilon_1 & -\varepsilon_2 & -\varepsilon_3 \end{bmatrix}, \tag{8}$$

with the quaternion vector component defined by $\boldsymbol{\varepsilon} = (\varepsilon_1, \varepsilon_2, \varepsilon_3)^{\mathrm{T}}$. The dynamic differential equation is expressed as function of the angular velocity vector, $\boldsymbol{\omega}$, the satellite inertia tensor, $\mathbf{I}_b$ (excluding the inertia of the reaction wheels around their rotation axes) with respect to the center

of mass, and the external torques, composed by the magnetic dipole disturbance $\mathbf{g}_{md}$, and the magnetic control torque $\mathbf{g}_{mc}$[14, 15]:

$$\mathbf{I}_b \dot{\boldsymbol{\omega}} = \mathbf{g}_{md} + \mathbf{g}_{mc} - \boldsymbol{\omega}^{\times} \left(\mathbf{I}_b \boldsymbol{\omega} + \mathbf{h}_w \right) - \mathbf{g}_w , \tag{9}$$

where $\mathbf{h}_w$ and $\mathbf{g}_w$ are respectively the reaction wheel angular momentum and control torque, both with respect to the satellite center of mass. The wheel's differential equation of motion is given by

$$\dot{\mathbf{h}}_w = \mathbf{g}_w . \tag{10}$$

The kinematic and dynamic equations were numerically integrated in simulation using the satellite simulator toolbox PROPAT[16]. The RW speed can be easily computed from the angular momentum with

$$\mathbf{I}_w \mathbf{w}_w = \mathbf{h}_w - \mathbf{I}_w \boldsymbol{\omega} , \tag{11}$$

in case the rotation axis of the three wheels are aligned to the body fixed axes. $\mathbf{I}_w$ is a diagonal matrix whose elements are the wheel's inertia around their rotation axes, and $\mathbf{w}_w$ is a vector whose components are the wheel speeds. The satellite full inertia, $\mathbf{I}$, including the wheels, is simply given by $\mathbf{I} = \mathbf{I}_b + \mathbf{I}_w$.

Kalman Filter With Reduced Covariance Matrix

The Kalman filter state is composed by the attitude quaternion $\mathbf{q}$ and the gyroscope bias vector $\mathbf{b}$, which will be estimated using the Reduced Order Covariance Method[9]. The state is thus given by

$$\mathbf{x} = \begin{pmatrix} \mathbf{q} \\ \mathbf{b} \end{pmatrix}, \tag{12}$$

whose differential equations of motion are[9]

$$\begin{aligned} \dot{\mathbf{q}} &= \frac{1}{2} \boldsymbol{\Omega}(\boldsymbol{\omega})\, \mathbf{q} = \frac{1}{2} \boldsymbol{\Omega}(\boldsymbol{\omega}_g - \mathbf{b})\, \mathbf{q} - \frac{1}{2} \boldsymbol{\Xi}(\mathbf{q})\, \boldsymbol{\eta} \\ \dot{\mathbf{b}} &= \boldsymbol{\mu} \end{aligned} \tag{13}$$

In this formulation, the state is seven-dimensional (four dimensions associated with the quaternion and three with the bias vector), and since the quaternion norm is unitary, i.e. $\mathbf{q}^T \mathbf{q} = 1$, then the state covariance $\mathbf{P}(t)$ becomes singular. Reference 9 suggests three different methods by which the state or just the covariance matrix can be reduced to order 6. The first of these methods is known as the reduced order representation of the covariance matrix and will be used in this work. The original formulation will not be presented here, but instead an equivalent formulation in which all matrix products involving a null or an identity matrix were removed, and thus optimizing the equations for onboard programming.

Details of the Kalman filter theory can be found in general[18, 19, 20] and specific[9, 17] literatures. In the sequence, a circumflex over a variable, as in $\hat{\mathbf{x}}$, indicates a value estimated by the filter, while a bar, such as in $\bar{\mathbf{x}}$ means a propagated or predicted variable. When the expectation operator is applied to the bias differential equation, the average noise becomes null and thus the mean bias

results constant during the time interval between two successive discrete filter evaluations. It follows that the estimation of the angular velocity is obtained by

$$\hat{\boldsymbol{\omega}}_k = \boldsymbol{\omega}_g - \hat{\mathbf{b}}_{k-1}, \tag{14}$$

such that $\hat{\mathbf{b}}_0 = \mathbf{0}$ can be assumed. Since the quaternion kinematics is linear, there is an analytic solution to the differential equation given by the quaternion transition matrix, $\boldsymbol{\Phi}_{k,k-1}$, in the interval t_{k-1} e t_k. After applying the expectation operator on Equation (13), the propagated quaternion results

$$\bar{\mathbf{q}}_k = \boldsymbol{\Phi}_{k,k-1}\, \hat{\mathbf{q}}_{k-1}, \tag{15}$$

and assuming that $\boldsymbol{\omega}(t)$ remains constant during the time interval, the transition matrix can be obtained by[9, 14]

$$\boldsymbol{\Phi}_{k,k-1} = \cos(|\,\Delta\boldsymbol{\theta}\,|/2)\,\mathbf{I} + \frac{\sin(|\,\Delta\boldsymbol{\theta}\,|/2)}{|\,\Delta\dot{\boldsymbol{\theta}}\,|}\,\boldsymbol{\Omega}(\Delta\boldsymbol{\theta}), \tag{16}$$

valid only for small increment angles $\Delta\boldsymbol{\theta} = \hat{\boldsymbol{\omega}}_k\, \Delta t$, where $\Delta t = t_k - t_{k-1}$. It should be noted that for small rotation angles, all the Euler sequence of rotation are equivalent. It also follows from the condition that the angular rate does not change from t_{k-1} to t_k that

$$\bar{\mathbf{b}}_k = \hat{\mathbf{b}}_{k-1}. \tag{17}$$

Equations (15) and (17) are the state prediction expressions. The reduced covariance matrix is defined by a transform of the full covariance matrix, where the transformation matrix $\boldsymbol{\Xi}(\hat{\mathbf{q}}_k)$ is function of the estimated attitude quaternion[9]. To avoid unnecessary null or identity products on the prediction of the state covariance matrix, the 6th order reduced matrix is partitioned in four 3rd order square matrixes, namely $\underline{\hat{\mathbf{P}}}_{k,11}$, $\underline{\hat{\mathbf{P}}}_{k,12}$, $\underline{\hat{\mathbf{P}}}_{k,21}$ and $\underline{\hat{\mathbf{P}}}_{k,22}$, in which the underscore bar means the reduced covariance, whereas

$$\hat{\mathbf{P}}_k = \begin{bmatrix} \boldsymbol{\Xi}\, \underline{\hat{\mathbf{P}}}_{k,11}\, \boldsymbol{\Xi}^{\mathrm{T}} & \boldsymbol{\Xi}\, \underline{\hat{\mathbf{P}}}_{k,12} \\ \underline{\hat{\mathbf{P}}}_{k,21}\, \boldsymbol{\Xi}^{\mathrm{T}} & \underline{\hat{\mathbf{P}}}_{k,22} \end{bmatrix} \tag{18}$$

is the full 7th order covariance matrix. Prediction of the covariance needs the attitude matrix between the last estimated quaternion $\hat{\mathbf{q}}_{k-1}$ and the predicted quaternion, $\bar{\mathbf{q}}_k$, which can be obtained either by the reduced transition matrix, given by

$$\underline{\boldsymbol{\Phi}}_{k,k-1} = \boldsymbol{\Xi}^{\mathrm{T}}(\bar{\mathbf{q}}_k)\, \boldsymbol{\Phi}_{k,k-1}\, \boldsymbol{\Xi}(\hat{\mathbf{q}}_{k-1}), \tag{19}$$

or by the attitude transform matrix

$$\underline{\boldsymbol{\Phi}}_{k,k-1} = \mathbf{A}(\bar{\mathbf{q}}_k)\, \mathbf{A}^{T}(\hat{\mathbf{q}}_{k-1}), \tag{20}$$

in which

$$\mathbf{A}(\mathbf{q}) = (\eta^2 - \boldsymbol{\varepsilon}^{\mathrm{T}}\boldsymbol{\varepsilon})\,\mathbf{1} + 2\,\boldsymbol{\varepsilon}\,\boldsymbol{\varepsilon}^{\mathrm{T}} - 2\,\eta\,\boldsymbol{\varepsilon}^{\times}. \tag{21}$$

and **1** is the 3rd order identity matrix. The predicted covariance needs also to integrate the Riccati equation that depends on the integral of the reduced transition matrix:

$$\underline{\mathbf{J}}_{k,k-1} = -\frac{1}{2}\int_{k-1}^{k} \underline{\mathbf{\Phi}}_{k,t}\, \mathrm{d}t\,. \tag{22}$$

It is assumed that $\underline{\mathbf{\Phi}}$ varies linearly in the time interval, which takes to

$$\underline{\mathbf{J}}_{k,k-1} = -\frac{1}{4}\left(\mathbf{1} + \underline{\mathbf{\Phi}}_{k,k-1}\right)\Delta t\,. \tag{23}$$

The same approach was employed to integrate the four reduced covariance matrices from the Riccati equation[9], resulting for the predicted covariance, after neglecting the higher order terms in Δt:

$$\begin{aligned}
\overline{\underline{\mathbf{P}}}_{k,11} &= \underline{\mathbf{\Phi}}_{k,k-1}\,(\hat{\underline{\mathbf{P}}}_{k-1,11} + \tfrac{1}{8}\mathbf{N}\,\Delta t)\,\underline{\mathbf{\Phi}}^{\mathrm{T}}_{k,k-1} + \underline{\mathbf{\Phi}}_{k,k-1}\,\hat{\underline{\mathbf{P}}}_{k-1,12}\,\underline{\mathbf{J}}^{\mathrm{T}}_{k,k-1} + \\
&\quad + \underline{\mathbf{J}}_{k,k-1}\,\hat{\underline{\mathbf{P}}}_{k-1,21}\,\underline{\mathbf{\Phi}}^{\mathrm{T}}_{k,k-1} + \underline{\mathbf{J}}_{k,k-1}\,(\hat{\underline{\mathbf{P}}}_{k-1,22} + \tfrac{1}{2}\mathbf{M}\,\Delta t)\,\underline{\mathbf{J}}^{\mathrm{T}}_{k,k-1} + \tfrac{1}{8}\mathbf{N}\,\Delta t \\
\overline{\underline{\mathbf{P}}}_{k,12} &= \underline{\mathbf{\Phi}}_{k,k-1}\,\hat{\underline{\mathbf{P}}}_{k-1,12} + \underline{\mathbf{J}}_{k,k-1}\,(\hat{\underline{\mathbf{P}}}_{k-1,22} + \tfrac{1}{2}\mathbf{M}\,\Delta t) \\
\overline{\underline{\mathbf{P}}}_{k,21} &= \hat{\underline{\mathbf{P}}}_{k-1,21}\,\underline{\mathbf{\Phi}}^{\mathrm{T}}_{k,k-1} + (\hat{\underline{\mathbf{P}}}_{k-1,22} + \tfrac{1}{2}\mathbf{M}\,\Delta t)\,\underline{\mathbf{J}}^{\mathrm{T}}_{k,k-1} \\
\overline{\underline{\mathbf{P}}}_{k,22} &= \hat{\underline{\mathbf{P}}}_{k-1,22} + \mathbf{M}\,\Delta t
\end{aligned} \tag{24}$$

The measurement vector is composed by the three-axis magnetometer and coarse sun sensor readings. It is assumed that the CSS outputs were previously processed in order to achieve the unit vector of the Sun direction in body frame coordinates. So the measurement vector has 6 dimensions, and therefore a 6th order matrix should be inverted to compute the Kalman gain. To avoid the computational effort of this inversion, filter updating will be done individually for each sensor axis. This is only valid if the sensor outputs are uncorrelated, which is true in this case, mainly if calibration procedures on the sensors are performed prior satellite launching. The observation error covariance matrix **R** becomes diagonal whose elements r_i are the squared standard deviation of the measures. Quite obvious is to perform scalar filter updating, since a 6 degree matrix inversion can be avoid, and thus covariance updating can be done for each sensor axis. However, the formulation of the sensitivity matrix **H** was not shown in Reference 9, but some guidelines on how to derive the 6 × 1 reduced sensitivity matrix were presented for the body-fixed covariance representation. It is assumed that the sensors were previously calibrated so the sensor models are simply the vectors of the geomagnetic field and Sun direction, in body-fixed frame, added to a non correlated Gaussian noise with standard deviation given by r_i, with i = 1, 2, …, 6. The sensitivity matrix for each axis at time t_k, $\mathbf{H}_{i,k}$ becomes now a row matrix given by

$$\mathbf{H}_{i,k} = \left(\frac{\partial}{\partial \mathbf{q}} s_i \quad \mathbf{0}\right)_{\bar{\mathbf{q}}_k} = \left(\mathbf{h}_{i,k} \quad \mathbf{0}\right), \tag{25}$$

where s_i gives the components of the two reference vectors in body coordinates, obtained from models of the magnetic field and Sun direction. s_i is computed from[9]

$$s_i = \mathbf{t}_i\; \mathbf{A}(\bar{\mathbf{q}}_k)\, \mathbf{p}_r\,, \tag{26}$$

with $\mathbf{p}_r$ being either the geomagnetic field or the Sun direction in the attitude reference frame, and $\mathbf{t}_i$ is the i^{th} sensor axis direction vector in body fixed frame, normally aligned to the satellite axes. The sensitivity row vector $\mathbf{h}_{k,i}$ results then

$$\mathbf{h}_{i,k} = 2\,\mathbf{t}_i\,\boldsymbol{\Xi}^{\mathrm{T}}(\bar{\mathbf{q}}_k)\,\boldsymbol{\Gamma} \tag{27}$$

where the matrix $\boldsymbol{\Gamma}$ is obtained from

$$\boldsymbol{\Gamma} = \left(\begin{array}{c|c} \mathbf{p}_r^{\times} & \mathbf{p}_r \\ \hline -\mathbf{p}_r^{\mathrm{T}} & 0 \end{array}\right). \tag{28}$$

The reduced order sensitivity row vector is given by

$$\underline{\mathbf{h}}_{i,k} = 2\,\mathbf{t}_i\,\boldsymbol{\Xi}^{\mathrm{T}}(\bar{\mathbf{q}}_k)\,\boldsymbol{\Gamma}\,\boldsymbol{\Xi}(\bar{\mathbf{q}}_k)\,, \tag{29}$$

and now the scalar $f_{i,k}$ can be obtained by

$$f_{i,k} = \underline{\mathbf{h}}_{i,k}\,\underline{\bar{\mathbf{P}}}_{i,k,11}\,\underline{\mathbf{h}}_{i,k}^{\mathrm{T}} + r_i\,, \tag{30}$$

which can be easily inverted. The reduced covariance matrices have now the additional index i to allow incremental updating. The reduced order Kalman gain for quaternion and gyroscope bias, $\underline{\mathbf{K}}_{i,kq}$ and $\underline{\mathbf{K}}_{i,kb}$, are computed from

$$\begin{aligned} \underline{\mathbf{K}}_{i,kq} &= \underline{\bar{\mathbf{P}}}_{i,k,11}\,\underline{\mathbf{h}}_{i,k}^{\mathrm{T}}\,f_{i,k}^{-1} \\ \underline{\mathbf{K}}_{i,kb} &= \underline{\bar{\mathbf{P}}}_{i,k,21}\,\underline{\mathbf{h}}_{i,k}^{\mathrm{T}}\,f_{i,k}^{-1} \end{aligned}, \tag{31}$$

and the reduced covariance updating is done with

$$\begin{aligned} \underline{\bar{\mathbf{P}}}_{i,k,11} &= \underline{\bar{\mathbf{P}}}_{i-1,k,11} - \underline{\mathbf{K}}_{i,kq}\,\underline{\mathbf{h}}_{i,k}\,\underline{\bar{\mathbf{P}}}_{i-1,k,11} \\ \underline{\bar{\mathbf{P}}}_{i,k,12} &= \underline{\bar{\mathbf{P}}}_{i-1,k,12} - \underline{\mathbf{K}}_{i,kq}\,\underline{\mathbf{h}}_{i,k}\,\underline{\bar{\mathbf{P}}}_{i-1,k,12} \\ \underline{\bar{\mathbf{P}}}_{i,k,21} &= \underline{\bar{\mathbf{P}}}_{i-1,k,21} - \underline{\mathbf{K}}_{i,kb}\,\underline{\mathbf{h}}_{i,k}\,\underline{\bar{\mathbf{P}}}_{i-1,k,21} \\ \underline{\bar{\mathbf{P}}}_{i,k,22} &= \underline{\bar{\mathbf{P}}}_{i-1,k,22} - \underline{\mathbf{K}}_{i,kb}\,\underline{\mathbf{h}}_{i,k}\,\underline{\bar{\mathbf{P}}}_{i-1,k,22} \end{aligned}, \tag{32}$$

and such that $\underline{\bar{\mathbf{P}}}_{0,k,mn} = \underline{\bar{\mathbf{P}}}_{k,mn}$ and $\hat{\mathbf{P}}_{k,mn} = \underline{\bar{\mathbf{P}}}_{l,k,mn}$, where l is the number of available axis measurements: 6 if both the magnetometer and sun sensors are available, or 3 if the satellite is in the Earth's shadow. The state is updated for each sensor axis by means of the full Kalman gain, obtained from

$$\begin{aligned} \mathbf{K}_{i,kq} &= \boldsymbol{\Xi}(\bar{\mathbf{q}}_k)\,\underline{\mathbf{K}}_{i,kq} \\ \mathbf{K}_{i,kb} &= \underline{\mathbf{K}}_{i,kb} \end{aligned}, \tag{33}$$

and so the quaternion and gyro bias updating is achieved by

$$\begin{aligned} \bar{\mathbf{q}}_{i,k} &= \bar{\mathbf{q}}_{i-1,k} + \mathbf{K}_{i,kq}[p_i - \mathbf{t}_i\,\mathbf{A}(\bar{\mathbf{q}}_k)\,\mathbf{p}_r] \\ \bar{\mathbf{b}}_{i,k} &= \bar{\mathbf{b}}_{i-1,k} + \mathbf{K}_{i,kb}[p_i - \mathbf{t}_i\,\mathbf{A}(\bar{\mathbf{q}}_k)\,\mathbf{p}_r] \end{aligned}, \tag{34}$$

where p_i is the sensor measurement associated with axis i, with initial and final conditions given by $\bar{\mathbf{q}}_{0,k} = \bar{\mathbf{q}}_k$, $\bar{\mathbf{b}}_{0,k} = \bar{\mathbf{b}}_k$, and $\hat{\mathbf{q}}_k = \bar{\mathbf{q}}_{l,k}$, $\hat{\mathbf{b}}_k = \bar{\mathbf{b}}_{l,k}$. It should be mentioned that the filtering equations does not preserves the quaternion unity, so quaternion normalization is needed just after the updating process.

Simulated Attitude Estimation

The algorithm for the reduced covariance Kalman filter was verified by simulation, using the PROPAT[16] toolbox to propagate the rigid body attitude and orbit. It was adopted a sun-synchronous orbit of 630 km altitude and 98° inclination. The geomagnetic field was simulated with IGRF-11[21], and the Sun direction was computed with 1' arc accuracy. Sensor noises were consistent with characteristics of the real sensors. Moreover, misalignments and scale factor was also considered in simulated measures. On the onboard computer the reference vector for the Earth's magnetic field will be calculated with a version of IGRF-11 expanded to 6th order, and the orbit will be propagated with SGP4[22]. The Two-Line Element set of the orbital elements after orbit injection will be retrieved from Celestrack[23]. Time interval of 1 sec was adopted for both attitude filtering and control. Attitude sensor readings will be averaged during this interval prior to Kalman filtering. However, the high noise of the gyroscopes makes the angular velocity still very noisy; thus the filtered velocity will pass to a digital first-order low pass filter before being utilized by the control algorithm. Figure 3 shows the attitude error of the Kalman filter, for an attitude representation in Euler axis and angle[14, 15]. The filter converges to the satellite attitude after 5 hours (~ 3 orbits), with a mean steady error around 10°. This error can be considered very large, but it's not surprising since the MEMS sensors are quite noisy. In fact, simulation has shown that the Kalman filter didn't manage to track the bias instability. The reason is that the gyroscope noise (0.182°/s standard deviation) is too high when compared with the bias instability (0.003°/s^2). As consequence, the estimated mean bias remains close to zero, far from the simulated value. The large peak attitude error shown in Figure 3, higher than the 50° after filter convergence, probably is due the lack of control in ADE that keeps the angular rate almost unchanged during simulation. As will be shown in next section, this error remains below 20° in the controlled modes.

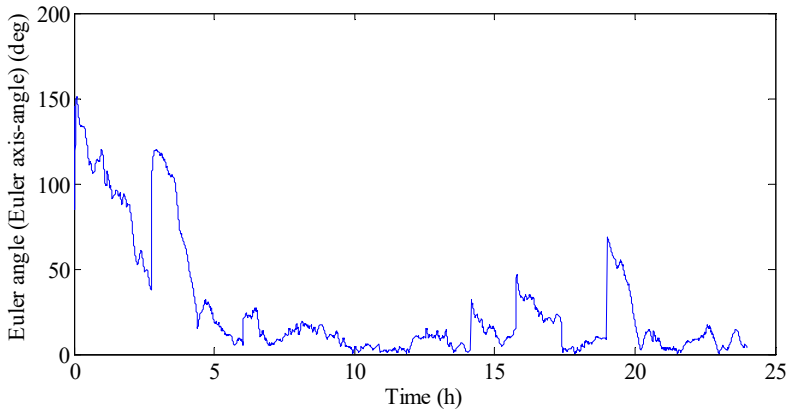

Figure 3. Estimated attitude error of the Kalman filter.

ATTITUDE CONTROL WITH REACTION WHEELS

Both nominal attitude control modes aim to point the satellite yaw axis to Earth and to keep the angular rate small with respect to the orbital reference frame. Due to limitations on the energy available for the ADCS, the reaction wheels can not be operated the whole orbit. So switching to RWC mode will be required whenever the satellite needs fine Earth pointing to acquire pictures, for instance. This can be done only when the satellite is in contact with mission center, which restricts the RWC to only few minutes per orbit. For the remaining part of the orbit the three-axis Magnetic Control Mode (MCM) will be employed. This will be shown in next section.

When in fine pointing mode, the wheel's speeds need to be damped by a magnetic control law. The block diagram of the RWC mode is shown in Figure 4. The controller computes the attitude error in Euler angles from the estimated attitude quaternion, besides the satellite angular velocity, with respect to the orbital frame, and applies a conventional *PD* (Proportional and Derivative) controller, which, in turn, commands the torque to the reaction wheels. The magnetic controller takes the wheel speed and applies just a proportional gain to drive the Magnetic Torque coils (MT) to keep the wheel speed inside the specified range.

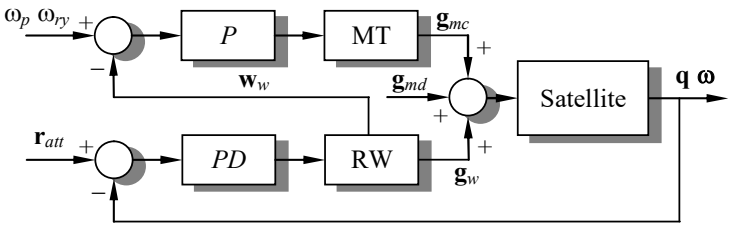

Figure 4. Block diagram of the RWC operating mode.

The RW was modeled with a dead band of 5.4 10^{-5} Nms angular momentum around the zero speed, according to data from supplier, besides a torque and speed hardware limits. This dead band affects negatively the attitude stabilization and pointing accuracy, mainly if the speed damping strategy tries to keep the angular rate close to zero. A simulation of the RWC mode was done using the Kalman filter to estimate the attitude and a low pass filter on the filtered satellite angular rate. The gyro model considers a bias, the bias drift, a Gaussian noise, scale factor errors and axis crossover. A simple average filter was applied to the simulated gyro measurements prior to Kalman filtering. The magnetometer and analog sun sensor models are based on Gaussian noise, scale factor errors and cross-axis coupling only. On Earth shadow the attitude is still estimated using magnetometer but with loss of accuracy. The proportional magnetic control to unload the RW momentum is composed of two individual controllers: the first one adjust the speed of the pitch wheel, and the second controls the speed of the wheels in roll and yaw axes. So it is possible not only to damp the wheel's speed, but also to set a non null angular rate on pitch axis and in the roll-yaw plane. If ω_p and ω_{ry} are the required angular rate of the reaction wheels in pitch axis and in the roll-yaw plane, respectively, then the desired torque in the pitch axis is given by

$$u_p = k_{mp}\,(w_3 - \omega_p)\,, \tag{35}$$

where $\mathbf{w}_w = (w_1 \;\; w_2 \;\; w_3)^{\mathrm{T}}$ are the RW angular rates in the yaw, roll and pitch axes, and k_{mp} is the pitch control gain. Once this torque shall lie in the pitch axis, then the magnetic moment on the yaw and roll torque coils will be calculated by

$$\begin{aligned} m_1 &= -u_p B_2 / |\mathbf{B}| \\ m_2 &= u_p B_1 / |\mathbf{B}| \end{aligned}, \tag{36}$$

in which $\mathbf{B} = (B_1 \;\; B_2 \;\; B_3)^T$ is the Earth's magnetic field in body fixed coordinates measured by the magnetometer. Defining $\mathbf{w}_{ry} = (w_1 \;\; w_2 \;\; 0)^T$ as the transverse angular rate of the wheels, the required torque on the roll-yaw plane will be

$$\mathbf{u}_{ry} = k_{mry} \left(1 - \frac{\omega_{ry}}{|\mathbf{w}_{ry}|} \right) \mathbf{w}_{ry}, \tag{37}$$

where k_{mry} is the roll-yaw plane control gain. This torque will be achieved by a magnetic moment on the pitch axis, calculated by means of

$$m_3 = k_{mry} \left(1 - \frac{\omega_{ry}}{|\mathbf{w}_{ry}|} \right) \frac{w_1 B_2 - w_2 B_1}{|\mathbf{B}|}, \tag{38}$$

Simulated Attitude Control With Reaction Wheels

Simulations of the RWC are shown in Figures 5 and 6. Figure 5 presents the attitude pointing error in Euler angle of a Euler axis and angle attitude representation for 10 hours (6 orbits, approximately). The red curve is the simulated attitude, while the blue is the estimated attitude by the Kalman filter. For a null attitude the Euler angle is zero and therefore the simulated attitude is also the attitude pointing error. The estimated attitude is small when compared with the simulated attitude, which means that the RWC manages to control the attitude with small error. On the other side, the estimation error is large, close to the simulated attitude. In other words, the satellite points precisely to a wrong direction, and therefore a mean error of 5° can be expected with the RWC mode. The reaction wheel speed and rate control is shown in Figure 6. It is noticeable on the roll-yaw curves the dead band of the reaction wheels during speed reversion. An angular momentum corresponding to a 200 rpm (≈ 21 rd/s) was commanded in the magnetic controller for both pitch axis and roll-yaw plane. It is also clear by comparing Figures 5 and 6 that the attitude error increases whenever the wheels revert their sense of rotation, which happens each ¼ of the orbit period. All the control gains were adjusted by simulation analysis, aiming to have a large gain margin and small steady pointing error.

MAGNETIC ATTITUDE CONTROL

Due to in orbit energy availability, the three-axis MCM will be the main attitude controller acting on satellite. The magnetic control is based on a *PID* controller that uses the CCPL[24] (Conventional Cross Product Law) to obtain the magnetic moment to be applied on the MT. The satellite magnetic dipole will be regulated by PWM (Pulse Width Modulation) acting on the coils. Since the magnetic control is unable to generate torque around the Earth's magnetic field, the applied torque shall be very small, just enough to compensate the disturbances on attitude. The slow variation of the Earth's field with respect to the orbit reference frame can be used to provide a mean torque in all three axes[24]. A relatively large derivative gain was chosen, to quickly decrease the satellite angular motion with respect to the orbital frame. The integral torque, on its turn, has to be very small and acts to compensate the external disturbances. The proportional gain is also small due to the reasons explained above.

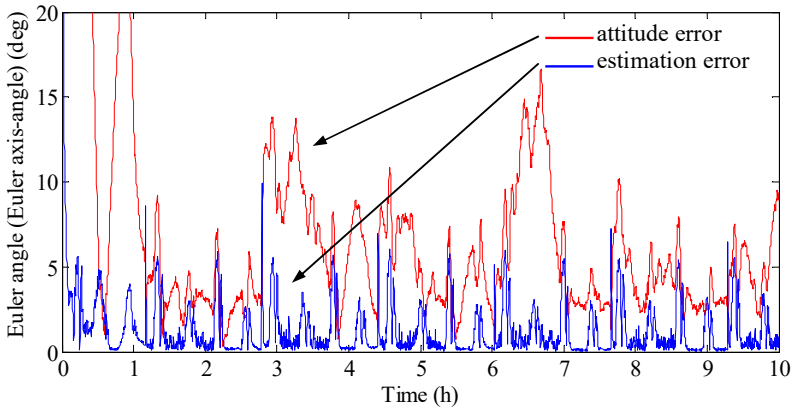

Figure 5. Satellite attitude error and estimation error.

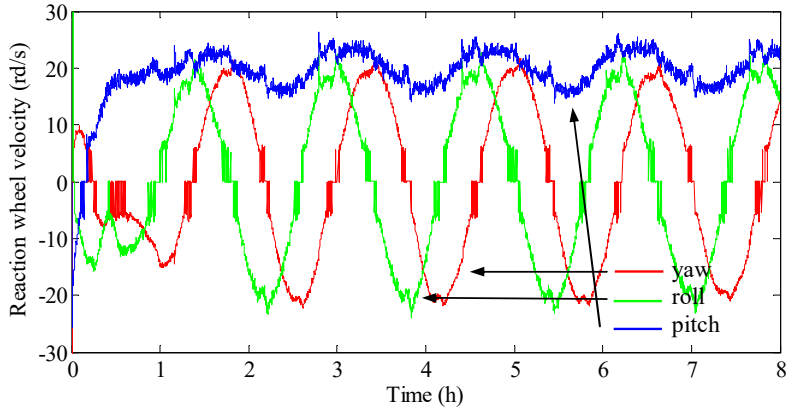

Figure 6. Reaction wheel angular rates.

The three-axis MCM is highly influenced by the noise coming from the sensors, particularly on the gyroscope. Due to the inability of the Kalman filter to track the gyroscope bias, the MCM error was still large in simulation, since the derivative gain must be high in order to keep the satellite angular rate close to zero. An alternative method was to compute the angular velocity directly from the attitude differential, which can be obtained from Equation (7):

$$\boldsymbol{\omega} = 2\,\boldsymbol{\Xi}^{\mathrm{T}}(\mathbf{q})\,\dot{\mathbf{q}}\,, \tag{39}$$

because it can be easily proved that $\boldsymbol{\Xi}^{\mathrm{T}}\,\boldsymbol{\Xi} = \mathbf{1}$. The differential is approximated by a finite difference of the quaternion estimated at time k and time k–1. It should be mentioned that the estimated quaternion depends on the gyroscope measurements, used by the Kalman filter. The filtered quaternion is significantly smoother than the attitude computed by a TRIAD or QUEST methods, but not so smooth to detect angular rates around 0.0001 rd/s necessary to control the attitude. So, a digital first order low pass filter with a cutoff frequency of 0.84 Hz was applied in

the computed angular rate to reduce the remaining noise. The differential angular rate based on the estimated quaternion can be calculated on the whole orbit, including the Earth shadow, whereas only in the sunlit orbit if the TRIAD was used instead.

Simulated Magnetic Attitude Control

To avoid unnecessary control action that happens when the control torque vector is almost aligned to the Earth's magnetic field, a dead band on the control was introduced, which turns off the coils whenever the angle between these vectors is less than 53°. This procedure not only improves control action but also reduces power consumption. Attitude error for MCM was calculated by Euler angles (yaw-roll-pitch) with respect to the orbital frame. A maximum duty-cycle of 50% was adopted for the PWM of the magnetic torque coils, to avoid sudden changes in control action. Control gains were adjusted aiming to get the lowest steady pointing error. However, some studies will be required in order to verify the control stability under different simulation parameters, like initial angular rate, orbit elements, sensor misalignments, scale factors and attitude disturbance torques. Figure 7 shows the simulated attitude of the three-axis magnetic attitude controller (red curve), in terms of the Euler angle, from a Euler axis and angle attitude representation[14, 15]. The Euler angle is zero only when the satellite body axes are parallel to the orbital system axes, and therefore the simulated attitude represents also the satellite pointing error. The blue curve is the estimation error, i.e., the Euler angle from the simulated to the estimated attitude. It is clear that the estimation error is significantly smaller than the attitude error, which means that the estimated attitude practically coincides with the simulated attitude, and also that the control error is still large when compared with the estimation error. From any initial attitude, the satellite reaches the final stabilization after 5 hours, approximately. The average error is still large, around 20°, but it is acceptable for this type of control. The magnetic stabilization and control is very sensitive to the residual magnetic dipole on the satellite. If the disturbance dipole could be reduced to 0.0001 instead of the estimated value of 0.001 Am^2, the mean pointing error would decrease to 5°. This means that a magnetic cleanliness on the satellite during integration shall be necessary in order to assure a small residual dipole.

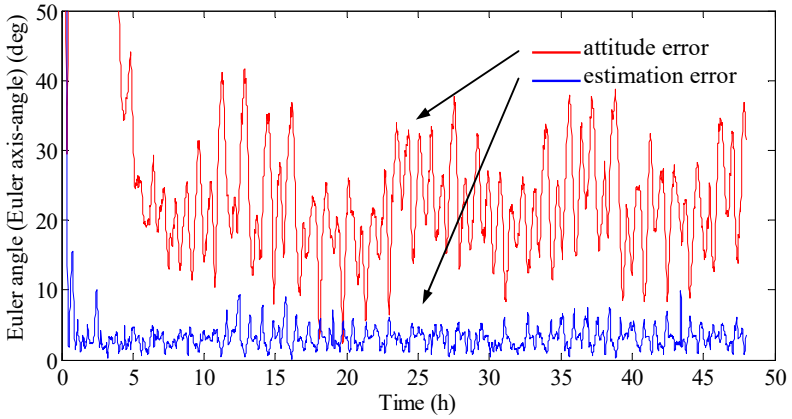

Figure 7. Attitude and estimation error of three-axis magnetic attitude control.

ATTITUDE STABILIZATION MODE

The purpose of the ASM is to damp the initial angular rate of the satellite, around 10 rpm just after launching separation, to a specified value close to 0.1 rpm, which is 10 times higher than the orbital angular rate. Two methods of magnetic attitude stabilization will be implemented, selectable by ground command: the B-dot and the Rate Reduction (RR). Both methods employ the cross product law to compute the control action, but in the RR the angular rate is provided by the gyroscopes instead of the magnetometer output differential used by the B-dot algorithm. Since the magnetic torque is given by the cross product between the coil magnetic moment and the Earth's field strength, as

$$\mathbf{g}_m = \mathbf{m}_{mag} \times \mathbf{B}, \tag{40}$$

so the magnetic moment vector can be obtained by

$$\mathbf{m}_{mag} = -k_{bdot} \frac{\dot{\mathbf{B}}}{|\mathbf{B}||\dot{\mathbf{B}}|}, \tag{41}$$

and remembering that by the time derivative of a vector in a rotating frame is such that

$$\dot{\mathbf{B}}\Big|_i = \dot{\mathbf{B}}\Big|_b + \boldsymbol{\omega} \times \mathbf{B}, \tag{42}$$

where the subscripts *i* and *b* mean the derivative taken in the inertial and body fixed frames, respectively, it results, after substituting Equations (42) and (41) in (40),

$$\mathbf{g}_m = \frac{k_{bdot}}{|\mathbf{B}||\dot{\mathbf{B}}|} (\boldsymbol{\omega} \times \mathbf{B}) \times \mathbf{B}, \tag{43}$$

considering, of course, that $\dot{\mathbf{B}}\Big|_i \ll \dot{\mathbf{B}}\Big|_b$ and therefore $\dot{\mathbf{B}}\Big|_i$ can be neglected. The resulting torque is opposed to the component of the angular rate perpendicular to the magnetic field **B**, and can decrease this component. Even considering that the component of **ω** in the direction of **B** can not be reduced, it will always be possible to generate torque in three-axis, although not at same time, since **B** changes slowly as the satellite travels its orbit.

The Rate Reduction algorithm is similar to the B-dot, except that it takes directly the satellite's angular rate as measured by the gyroscope, instead of the time derivative of the geomagnetic field, to compute the magnetic moment to be applied to the MT:

$$\mathbf{m}_{mag} = \frac{k_{rr}}{|\boldsymbol{\omega}_g||\mathbf{B}|} \boldsymbol{\omega}_g \times \mathbf{B}, \tag{44}$$

Simulated Attitude Stabilization

Both modes, B-dot and Rate Reduction, and gave similar results on simulation. The rotational kinetic energy of the satellite is shown in Figure 8. It can be seen that attitude stability is achieved in less than 7 hours after orbit injection, considering the required angular rate of 0.01 rd/s, which corresponds to a kinetic energy of 5 μJ, approximately. A constant residual magnetic moment of 0.001 Am2 magnitude on the satellite was considered as a single perturbation on attitude. A maximum dipole of 0.04 Am2 (20% of the maximum available) in each magnetic torque coil was

adopted to avoid fast control action, and to allow time for magnetometer readings without interference from the dipole generated by MT. There is no significant difference between the B-dot and the RR methods. The B-dot seems to be slower than the Rate Reduction, as expected, since $\dot{\mathbf{B}}$ only approximates the full angular rate $\boldsymbol{\omega}$. However the B-dot method can reach a lower final angular rate than the RR algorithm.

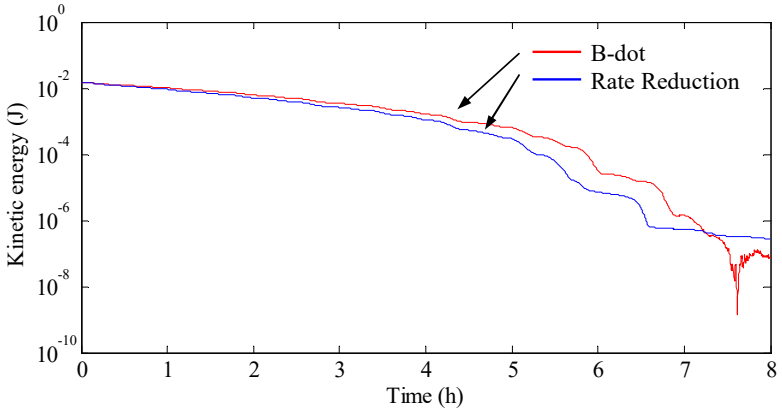

Figure 8. Attitude stabilization and angular rate damping.

CONCLUSION

This paper presented the Attitude Determination and Control System (ADCS) of ITASAT, a 6U form factor CubeSat. The attitude determination and estimation is based on two vectors measures, provided by a magnetometer and sun sensors, while the control is performed by a set of reaction wheels and magnetic torque coils. The ITASAT operation modes were presented, together with the attitude control laws that shall be used in each mode. A Kalman filter estimates the quaternion attitude and the gyroscope biases, or drift, in all operating modes. The filter was optimized for embedded computing, derived from the reduced order of the covariance matrix[9], suitable to avoid convergence problems if the matrix becomes singular. The expressions of the sensitivity matrix employ scalar sensor measurements in filter updating which eliminates the 6th order matrix inversion.

It is expected that the attitude control in fine pointing mode, with reaction wheels, will reach an average precision pointing around 5°, mainly due to attitude estimation error. Because the reaction wheels have a operating dead zone around the null angular momentum, a magnetic controller has been introduced to keep the angular speed of the wheels far off the dead zone. This strategy managed to keep the reaction wheels operating around a specified angular momentum, although the roll-yaw wheels exchange their angular rates in Earth pointing stabilization.

Due to the on-board power availability, the wheels shall not operate continuously, but alternately with a three-axis magnetic attitude control. The final pointing error achieved in simulation with the three-axis magnetic control (around 20°), showed a small gain margin, which indicates that this control is particularly susceptible to modeling errors and, therefore, the simulation may differ from in-orbit results. Contrary to the reaction wheel control mode, in this case the pointing error is mainly caused by the controller, since the average estimation error is less than 5°.

Two attitude stabilization methods to decrease the satellite angular velocity were simulated: the first was based on Bdot, and the second used the gyro measurements to compute the control torque. Both methods have shown to be equivalent from the performance perspective achieved in the simulation.

CubSats are promising platforms for developing new technologies, including the in-orbit qualification of ADCS systems. The proposed solution for the ITASAT attitude determination and control will be the first test of a three-axis ADCS software developed in Brazil, and the benefits coming from this knowledge can be used in large missions currently under development in that country.

ACKNOWLEDGMENTS

The author is thankful to Finep and the SIA (Inertial Systems for Aerospace Applications) project for the financial support.

REFERENCES

[1] H. D. Black, "A passive System for Determining the Attitude of a Satellite", AIAA Journal, Vol. 2, no. 7, 1964, pages 1350-1351.

[2] F. L. Markley, "Attitude Determination Using Two Vector Measurements", 1998, NASA Goddard Space Flight Center, Rept. 99-001. http://wayback.archive-it.org/1792/20100214090230/.

[3] F. L. Markley, "Attitude Determination Using Vector Observations: A Fast Optimal Matrix Algorithm", Journal of the Astronautical Sciences, Vol. 41, No. 2, 1993, pages 261-280.

[4] M. D. Shuster and S. D. Oh, "Three-axis Attitude Determination from Vector Observations", Journal of Guidance and Control, Vol. 4, No. 1, 1981, pages 70-77.

[5] F. L. Markley and D. Mortari, "Quaternion Attitude Estimation Using Vector Observations", AAS The Journal of the Astronautical Sciences, Vol. 48, No. 2/3, 2000, pp. 359-380.

[6] J. L. Crassidis and F. L. Markley, "Unscented Filtering for Spacecraft Attitude Estimation", Journal of Guidance, Control, and Dynamics, Vol. 26, No. 4, 2003, pp. 536-542.

[7] L. Cooper, D. Choukroun and N. Berman, "Spacecraft Attitude Estimation via Stochastic H_∞ Filtering", AIAA Guidance, Navigation and Control Conference, Toronto, Canada, 2010, AIAA paper 2010-8340.

[8] F. L. Markley and J. L. Crassidis, "Fundamentals of Spacecraft Attitude Determination and Control", Springer, 2014, ISBN 978-1-4939-0802-8.

[9] E. J. Lefferts, F. L. Markley and M. D. Shuster, "Kalman Filtering for Spacecraft Attitude Estimation", Journal of Guidance, Vol. 5, No. 5, 1982, pages 417-429.

[10] X. Yun, E. R. Bachmann and R. B. McGhee, "A Simplified Quaternion-Based Algorithm for Orientation Estimation From Earth Gravity and Magnetic Field Measurements", IEEE Transactions on Instrumentation and Measurement, Vol. 57, No. 3, 2008, pages 638-650.

[11] Vladimir A. Bushenkov, Michael Yu. Ovchinnikov, Georgi V. Smirnov: Attitude Stabilization of a Satellite by Magnetic Coils, Acta Astronautica, Vol. 50, No. 12, 2002, pages 721-728.

[12] D. Allan, "Statistics of Atomic Frequency Standards", Proceedings of IEEE, Vol. 54, No 2, 1966, pages 221–230.

[13] Freescale Semiconductor, "Allan Variance: Noise Analysis for Gyroscopes", Freescale Application Note AN5087, 2015. < http://cache.freescale.com/files/sensors/doc/app_note/AN5087.pdf>

[14] J. R. Wertz, "Spacecraft Attitude Determination and Control", London, D. Reidel, Astrophysics and Space Science Library, 1978.

[15] P. C. Hughes, "Spacecraft Attitude Dynamics", Mineola, Dover, 1986.

[16] V. Carrara: *An Open Source Satellite Attitude and Orbit Simulator Toolbox for Matlab*, 2015, Proceedings of the XVII International Symposium on Dynamic Problems of Mechanics. Natal, RN, Brazil, Feb 22-27, (ISSN 2316-9567).

[17] J. L. Crassidis, F. L. Markley, and Y. Cheng, "A Survey of Nonlinear Attitude Estimation Methods," AIAA Journal of Guidance, Control, and Dynamics, Vol. 30, No. 1, 2007, pages 12-28.

[18] R. E. Kalman, "A New Approach to Linear Filtering and Prediction Problems", Journal of Basic Engineering, Vol. 82, No. 35, 1960.

[19] A. H. Jazwinski, "Stochastic processes and filtering theory", Academic Press, New York, 1970. ISBN 0-12-381550-9.

[20] A. Gelb, "Applied Optimal Estimation", Cambridge, MA, M.I.T. Press, 1974.

[21] International Association of Geomagnetism and Aeronomy, "International Geomagnetic Reference Field", 2015, <http://www.ngdc.noaa.gov/IAGA/vmod/ igrf.html>.

[22] F. R. Hoots and R. L. Roehrich, "Models for Propagation of NORAD Element Sets", Spacetrack Report No. 3, Aerospace Defense Center, Peterson AFB, 1980.

[23] T. S. Kelso, "Celestrack NORAD Two-Line Element Sets – Current Data", 2015, <http://www.celestrak.com/NORAD/elements/>.

[24] P. J. Camillo and F. L. Markley, "Orbit-averaged behavior of magnetic control laws for momentum unloading", Journal of Guidance, Control, and Dynamics, Vol. 3, No. 6, 1980, pages 563-568.